Fermi National Accelerator Laboratory

Measurement of the Mass of the B_s^0 Meson in p̄p Collisions at $\sqrt{s}$ = 1.8 TeV

F. Abe et al.

The CDF Collaboration

Fermi National Accelerator Laboratory
P.O. Box 500, Batavia, Illinois 60510

July 1995

Disclaimer

Measurement of the Mass of the B_s^0 Meson in $\overline{p}p$ Collisions at $\sqrt{s} = 1.8$ TeV

The CDF Collaboration [1]

Abstract

We measure the mass of the B_s^0 meson by fully reconstructing the decay $B_s^0 \to J/\psi \; \phi$ with the subsequent decays $J/\psi \to \mu^+ \; \mu^-$ and $\phi \to K^+ \; K^-$. The data was obtained from 19.3 pb^{-1} of integrated luminosity of $\overline{p}p$ collisions at $\sqrt{s} = 1.8$ TeV using the Collider Detector at Fermilab (CDF). A sample of 80,000 inclusive $J/\psi \to \mu^+ \; \mu^-$ events is used to study systematic biases in track reconstruction and is used to calibrate the momentum scale. We reconstruct the kinematically similar decays $B^- \to J/\psi \; K^-$ and $B^0 \to J/\psi \; K^*$ to study the mass measurement technique used for the B_s^0 meson. Based on the observation of 32 ± 6 candidates, the mass of the B_s^0 meson is measured to be $5369.9 \pm 2.3 \pm 1.3$ MeV/c^2.

---

[1]Contributed paper to the 17th International Symposium on Lepton-Photon Interactions, Beijing, China, Aug 10-15, 1995.

1 Introduction

The Fermilab Tevatron and the Collider Detector at Fermilab (CDF) provide a rich environment for making measurements using fully reconstructed B hadrons [1]. The total cross section for $b\bar{b}$ production at the Fermilab Tevatron is about 50 μb [2, 3]. In the 1992-1993 CDF run, the integrated luminosity of 19.3 pb^{-1} implies that roughly 10^9 $b\bar{b}$ pairs were produced inside the CDF detector. A fraction of these events passed trigger requirements and were recorded to tape for analysis because the bottom hadron decayed into a J/ψ with the subsequent decay $J/\psi \to \mu^+ \mu^-$. The J/ψ events arise both from charmonium production and from decays of B hadrons. When the J/ψ is from a B hadron decay, the relatively massive J/ψ in the final state makes it more probable that the B has decayed into a relatively few charged final state particles. The J/ψ event sample is hence enriched with reconstructible B decays and measurements based on samples of reconstructed exclusive final states may be made.

This paper updates the CDF result of Ref. [4] using the entire 1992-1993 data sample with improved track reconstruction. The current world average mass of the B_s^0 meson is 5375 $\pm$ 6 MeV/c^2 [5] which includes the value obtained by Ref. [4] and by experiments performed at LEP [6].

2 Detector

The CDF detector has been described in detail elsewhere [7, 8]. It is shown schematically in Fig. 1. A silicon vertex detector (SVX) [9] consisting of four layers of silicon strip detectors located between radii of 2.9 and 7.9 cm and extending $\pm$ 25 cm in z from the center of the detector provides spatial measurements for charged tracks with a resolution of 13 μm in the r-ϕ plane [10]. The geometric acceptance for the SVX is $\sim$ 60% as the interactions are distributed along the beam axis with a RMS width of $\sim$ 30 cm. Surrounding the SVX is a time projection chamber (VTX) which provides tracking measurements in the r-z plane. The VTX is used in this analysis to provide the event vertex position in z. Momenta of charged particles are measured in three dimensions by the central tracking chamber (CTC), an 84-layer drift chamber which covers the pseudorapidity interval $|\eta| < 1.1$ where $\eta = -\ln[\tan(\theta/2)]$. The 84 layers are divided into 9 alternating superlayers of 12-wire axial and 6-wire 3° stereo sense wires. The SVX, VTX, and CTC are located in an axial magnetic field with an average strength of 1.41 T. Electromagnetic and hadronic calorimeters are located outside the tracking volume. Muons are identified using three different subsystems each consisting of four layers of drift chambers. The central muon chambers (CMU), located behind $\sim$ 5 absorption lengths of calorimeter, cover 85% of ϕ in the range $|\eta| < 0.6$. Gaps in ϕ coverage are filled in part by the central upgrade muon chambers (CMP) with total coverage in ϕ of 85% and $|\eta| < 0.6$. These chambers are located behind a total of $\sim$ 8 absorption lengths. Finally, central extension muon chambers (CMX) provide 67% coverage in ϕ for the region 0.6 $< |\eta| <$ 1.0 behind $\sim$ 6 absorption lengths. The muon system provides the means for identifying and triggering on events with $J/\psi \to \mu^+ \mu^-$ decays. The large tracking volume and strong magnetic field provide excellent momentum resolution.

1

3 $J/\psi \rightarrow \mu^+ \mu^-$ Sample

3.1   Trigger

Dimuon events are collected using a three-level trigger. The Level 1 trigger re-
quires two muon chamber track segments with a nominal P_T larger than 3.3 GeV/c.
For most of the run, one of the muon segments is required to be in the CMU. At
Level 2, one of the two muon track segments is required to match a track in the
CTC found by a hardware fast track processor (CFT). If a CMX muon is involved,
it is required to have a matched CFT track. In addition, hadronic energy deposi-
tion in the calorimeter tower towards which the muon track pointed is required to
be larger than 0.5 GeV as expected for a minimum ionizing particle. In Level 3,
software event reconstruction is performed. Dimuon J/ψ candidates are selected
by imposing the requirement that two oppositely charged muons have extrapo-
lated CTC tracks matching muon chamber track segments to within 4 σ (based on
multiple scattering calculations). In addition, the invariant mass of the dimuon is
required to between 2.8 and 3.4 GeV/c^2.

3.2   Offline Reconstruction

Dimuon events which pass all three levels of trigger requirements are processed
offline using improved calibration constants and track reconstruction algorithms.
In the presence of a uniform axial magnetic field, a charged particle will travel in
a helical trajectory that can be described using five track parameters (cylindrical
coordinates): curvature (inverse diameter of the circle obtained by projecting the
helix in the r-ϕ plane), **crv**; impact parameter, d_0; ϕ_0; z_0; and $\cot\theta$ where the
subscript, 0 indicates that the parameter is with respect to the point of closest
approach to the nominal beam axis. The transverse momentum of a track is
inversely proportional to the curvature and is proportional to the nominal axial
magnetic field, B:

$$P_T = \frac{c}{2}\frac{\text{B}}{\mathbf{crv}} = \frac{\kappa}{\mathbf{crv}} \tag{1}$$

where c is the speed of light and κ is defined by the equation. Track candidates
are found in the CTC using road-based pattern recognition algorithms. Track
parameters of a given track are determined by fitting tracking chamber hits to
a trajectory of a helix which is perturbed because of small non-uniformities in
the magnetic field [12]. If a well-matched pattern of SVX hits is found when
extrapolating the CTC track into the SVX volume, those hits are included in
the fit generally improving the resolution of **crv**, d_0, and ϕ_0. In addition to
determining the five helical track parameters, the track fitting also determines
a covariance matrix which expresses measurement uncertainties of the five track
parameters and their correlations (including effects such as multiple scattering).
We multiply all of the elements of the covariance matrix by a factor of 1.8 so that
the CTC-SVX matching uncertainty agrees with the measured resolution. The
underestimation of the covariance matrix is due in part to the fact that multiple
scattering within the volume of the CTC (gas and wires) is not accounted for in
the track fitting procedure.

3.3 Final J/ψ Selection

For J/ψ reconstruction, the two muon tracks are constrained to come from a common vertex. The effect of this constraint is to improve the mass resolution as determined by a single Gaussian fit from 22 to 17 MeV/c^2. To select $J/\psi \rightarrow \mu^+ \mu^-$ candidates, a minimal set of selection criteria are used emphasizing efficiency. Matching between the extrapolated track and the hits in the muon chambers are required to be within 3 σ in r-ϕ and 3.5 σ in z for the CMU chamber where σ represents the expected uncertainty in extrapolation due to multiple scattering. These requirements remove approximately 10% of the background while preserving > 99% of the signal. Figure 2 shows the CDF dimuon mass spectrum. For B hadron reconstruction, J/ψ candidates are those dimuons with a vertex constrained dimuon mass within 100 MeV/c^2 of the world average J/ψ mass of 3096.93 MeV/c^2 [11].

4 Track Corrections and Momentum Scale

Compared with the results of Ref. [4], improvements in the offline reconstruction are made with the alignment of the SVX to the CTC, internal CTC calibration, and in using measured non-uniformities in the solenoidal magnetic field. High statistics studies with $J/\psi \rightarrow \mu^+ \mu^-$ decays and with high energy electrons, where energy and momentum are measured independently, are used to provide corrections to the reconstructed tracks. These improvements affect the overall mass resolution and also remove several systematic effects.

We will demonstrate using the high statistical precision afforded by the $J/\psi \rightarrow \mu^+ \mu^-$ decay sample that we are able to determine, on average, the momentum scale of charged particles. We first describe calibrations and corrections applied to the nominal CTC and SVX track reconstruction. We apply corrections motivated by observed systematic effects in the reconstructed J/ψ mass and in comparing the ratio of energy to momentum, E/P, for electron candidates. After these corrections have been made, we use the reconstructed J/ψ mass to determine the momentum scale. In the next section, we discuss B meson reconstruction at CDF.

4.1 CTC Calibration and False Curvature

The CTC is aligned and calibrated in several steps in order to determine the relationship between drift time and distance to a sense wire. Electronic pulsing calibrations are used to determine the relative time pedestal for each sense wire. Additional corrections from the data are applied if non-uniformities are found as a function of time. The individual wire positions are calibrated by requiring the ratio of energy to momentum, E/P, of high-P_T electrons, to be charge independent. After calibrations, the nominal CTC resolution is approximately 200 μm. The $J/\psi \rightarrow \mu^+ \mu^-$ sample can be used to illustrate the effect of these calibrations. Before the final alignment, a false curvature systematic effect $(\mathbf{crv}_{fitted} = \mathbf{crv}_{true} + \delta)$ was present as can be seen in studying the reconstructed J/ψ mass as a function of the difference in curvature between the positive and negative muon (Fig. 3).

After final alignment, there is no statistically significant remaining false curvature. It should be noted that for the case of a charge symmetric decay such as $B_s^0 \to J/\psi \phi$ with $J/\psi \to \mu^+ \mu^-$ and $\phi \to K^+ K^-$ (equal numbers of positively and negatively charged tracks with the same momentum spectrum in the final state), a false curvature systematic effect would worsen the resolution but result in no systematic shift in mass.

Electron candidates are measured both by the calorimeter and tracking chamber. The ratio of E/P for these candidates should not show a dependence over the detector geometry. In studies used by CDF to measure the W boson mass [13], systematic mismeasurements are observed where the fitted curvature is a a function of ϕ and $\cot\theta$. The following corrections were derived and are used in this analysis:

$$\delta(\mathbf{crv}) = -0.00025 \times \kappa \times \sin(\phi - \phi_0) \; (cm^{-1}) \tag{2}$$

$$\delta(\mathbf{crv}) = -0.00035 \times \kappa \times (\cot\theta + z_{vertex}/187) \; (cm^{-1}) \tag{3}$$

where ϕ_0 equals 3.6 radians and z_{vertex} is measured in cm. As these corrections average to zero over the detector geometry and there is no statistically significant asymmetry in B decays over the detector geometry, no systematic uncertainty is assigned for the B meson mass determination.

4.2 Corrections for Energy Loss

Corrections of track parameters due to dE/dx losses are based on extrapolating particles through a model of the known detector material from the particle's origin through the inner wall of the CTC (before the track is measured). Photon conversion data measures that this amount of material corresponds to $8.1 \pm 0.4\%$ radiation lengths. For $J/\psi \to \mu^+ \mu^-$ decays, without correcting for the energy loss, the unconstrained mass would be measured low by 5 ± 2 MeV/c^2 where the uncertainty is dominated by the incomplete knowledge of the composition of materials within the CTC volume. The uncertainty in the dE/dx correction dominates the momentum scale uncertainty and contributes to a systematic uncertainty in the B meson mass determination.

4.3 $\Delta \cot\theta$ Systematic Effect

The longitudinal momentum, P_z, is expressed in terms of P_T and the $\cot\theta$ track parameter.

$$P_z = P_T \cot\theta \tag{4}$$

Figure 4 shows the fitted J/ψ mass in bins of the difference in $\cot\theta$ for the two muons showing a large systematic effect (top). A correction is applied to scale $\cot\theta$ by 0.9985 which lessens any dependence (bottom). The root cause of this systematic effect is not completely understood. In evaluating systematic uncertainties, the correction 0.9985 will be modified by $\pm$ 0.0008 to estimate the systematic effect on measuring the masses of the B mesons. In Fig. 4, a slight slope as a function of $\Delta \cot\theta$ is observed after the correction is applied. A physical interpretation is a small twist between the two CTC endplates. This slope is within the bounds of the variation of the $\cot\theta$ scale factor used for evaluating systematic unceratinties shown by the dotted lines in Fig. 4.

4

4.4 Additional Studies for Systematic Tracking Effects

A number of additional studies using the high statistics J/ψ sample have been performed to examine possible systematic tracking effects. The reconstructed J/ψ mass as a function of time throughout the data taking period fluctuates about the mean with a component of 0.4 MeV/c^2 larger than expected based upon statistics alone. This fluctuation is larger than could be explained by monitored small magnetic field fluctuations. No systematic uncertainty is assigned because both the J/ψ mass and B meson mass reconstruction are averaged over the entire data taking period. Another check has been to look for a systematic effect in the J/ψ mass when a muon passes through the extreme edges of the tracking volume where residual magnetic field non-uniformities would be expected to be most prevalent. There is no observed statistically significant systematic effect. A systematic effect has been found due to a small mis-alignment of the axial magnetic field and detector axis. This effect causes no shift since it can be averaged over in ϕ. The mass difference between J/ψ reconstructed with and without the vertex constraint is centered about zero as is the mass difference between using and not using SVX information.

The reconstructed J/ψ mass has been examined as a function of the inverse $P_T{}^2$ averaged for the two muons (a possible higher order systematic effect in **crv**). There is no statistical evidence of a systematic effect over the P_T range probed by dimuons from J/ψ decay. The J/ψ muons probe down to a P_T of 1.4 GeV/c since muons of lower P_T are likely to be stopped within the calorimeter. In Section 6, possible systematic effects at lower P_T will be studied using $\psi(2S) \rightarrow J/\psi\ \pi^+\ \pi^-$ and $B^0 \rightarrow J/\psi\ K^*$ decays.

4.5 Momentum Scale

The overall momentum scale is set by requiring the reconstructed J/ψ mass to be equal to the world average. After the corrections which have been discussed, we find a J/ψ mass of 3096.5 MeV/c^2 which agrees well with the world average of 3096.93 MeV/c^2. The momentum scale is thus corrected larger by a factor of .015% This momentum scale correction is within expectations given the measurement precision of the average magnetic field value which is known to within 0.03%. The systematic uncertainty in establishing the momentum scale from the J/ψ mass arises from several effects. The dimuon mass is determined by a binned-likelihood fit of Fig. 2 to a Gaussian on a linear background distribution. The precision of setting the fitted mass to the world average is limited by the statistical uncertainty of the fit (0.1 MeV/c^2), the uncertainty in the world average (0.04 MeV/c^2 [11]), and the effect of the background shape (0.1 MeV/c^2). The fit corrects for *Bremsstrahlung* by adding a constant of 0.8 ± 0.2 MeV/c^2 to the resultant mass as determined by a Monte Carlo study of the process. Adding the uncertainties in quadrature gives a precision of 0.3 MeV/c^2 to which the measured dimuon mass can be set to the world average J/ψ mass. The uncertainty in the dE/dx correction contributes to the momentum scale uncertainty in so far as the reconstructed dimuon mass remains within the 0.3 MeV/c^2 precision of the J/ψ mass. Under an extreme variation of the dE/dx model, the J/ψ mass shifts lower by 0.9 MeV/c^2. A momentum scale increase of 0.02% would leave the

dimuon mass within 0.3 MeV/c^2 of the world average. Thus, 0.02% is taken as the uncertainty on the momentum scale due to the uncertainty in the energy loss correction. The overall momentum scale uncertainty is dominated by this effect and is taken to be 0.02%.

The momentum scale is checked by reconstructing $\Upsilon \to \mu^+ \mu^-$. Figure 5 shows the reconstructed $\Upsilon \to \mu^+ \mu^-$ with a binned likelihood fit to a Gaussian and second order polynomial. Including an additive correction of 3 ± 1 MeV/c^2 determined from Monte Carlo for *Bremsstrahlung*, we find the mass of the $\Upsilon(1S)$ to be $9459.6 \pm 2.2 \pm 1.0$ MeV/c^2 which agrees well with the world average mass of 9460.4 ± 0.2 MeV/c^2 [14]. The $\Upsilon(2S)$ and $\Upsilon(3S)$ states are also reconstructed at masses which agree with the world averages within our statistical precision.

5 B Meson Reconstruction

All charged tracks passing quality cuts are considered as pion and kaon candidates. These quality cuts require that the track be measured in three dimensions by the CTC and must have a minimum of 4 (2) associated hits on a minimum of 4 axial (2 stereo) superlayers. The daughter meson (K, K^*, or ϕ) in $B^- \to J/\psi \ K^-$, $B^0 \to J/\psi \ K^*$, and $B_s^0 \to J/\psi \ \phi$ decays is selected as follows. The K is any charged track. The K^* candidate consists of any two oppositely charged tracks that have an invariant mass in a $\pm$ 50 MeV/c^2 window around 896 MeV/c^2 when one track is assigned a kaon mass and one a pion mass. In the case where the opposite $K - \pi$ mass assignment also is consistent with being a K^*, only the candidate closest to the K^* mass is used. Monte Carlo studies allow us to estimate that this procedure is correct approximately 75% of the time with insignificant loss of mass resolution. A ϕ candidate consists of any two oppositely charged tracks which have an invariant mass within 10 MeV/c^2 of the ϕ mass. The narrowness of the ϕ resonance relative to the K^* reduces considerably the combinatoric background in the $B_s^0 \to J/\psi \ \phi$ search.

Combining all K, K^*, and ϕ candidates with the J/ψ results in large combinatorial backgrounds in the B meson mass region. These backgrounds are reduced relative to the respective signals using constrained fitting techniques to improve the mass resolution. In addition, selection criteria on the transverse momentum of the daughter and B mesons and on the proper lifetime improve signal-to-noise.

5.1 Constrained Fitting

The primary collision vertex in r-ϕ is determined by using SVX track measurements averaged over many events. The uncertainty is dominated by the beam spot size of $\sim$ 40 μm. The VTX provides the z primary vertex position event-by-event with a resolution of 500 μm.

When the respective tracks of the daughter mesons are combined with a J/ψ candidate, a simultaneous constraint is performed where the dimuons are constrained to have the J/ψ mass, all tracks originate from a common secondary vertex, and the momentum vector of the B candidate points back along the line from the secondary vertex to primary vertex in the r-ϕ plane. From the constrained fit, the secondary vertex is determined and the resolution of the track

parameters are improved. For $B^- \to J/\psi\ K^-$ reconstruction (see Fig. 6), the mass resolution as determined by the σ of a binned-Gaussian fit is improved from 37 to 14 MeV/c^2. In addition, a CL(χ^2) from the fit is calculated using the changes in the respective track parameters relative to measurement uncertainties. A requirement that CL(χ^2) > 1% removes combinatoric background associated with track candidates which are mismeasured.

5.2   Selection Criteria

Requirements imposed upon the transverse momenta of the daughter and of the reconstructed B mesons improve signal-to-noise of the reconstructed states. The selection criteria have been studied using the sideband-subtracted B meson signal regions to estimate (to within approximately 10%) the efficiency of the different requirements. The requirement that the transverse momentum of the reconstructed B meson candidate be larger than 6 (8) GeV/c given the kaon has a P_T above 2 GeV/c is 95 (80)% efficient for signal and only 60 (30)% efficient for combinatoric background.

The B mesons under study all have a lifetime of approximately 1.5 ps [15] which can be distinguished from a zero ps lifetime expected for tracks originating from the primary vetex. When the reconstructed B has at least two SVX tracks (true for approximately 50% of the candidates), the $c\tau$ resolution is ~ 50 μm (otherwise the resolution is nominally ~ 200 μm). For the case where at least two of the final state tracks have SVX information, the requirement that $c\tau > 0$ (100) μm is $\sim 85(70)$% efficient for signal and only $\sim 55(25)$% efficient for the background. When the secondary vertex is not measured by the SVX, a requirement of $c\tau > 0$ (100) μm is $\sim 70(60)$% efficient for signal and only $\sim 55(45)$% efficient for background. The looser requirement that $c\tau$ be positive is made for B^0_s candidates since the combinatoric background is relatively smaller due to the narrow window used to select ϕ candidates.

Table 1 summarizes the set of selection criteria which will be used for each of the reconstructed B mesons.

$B \to J/\psi\ X$ Decay	$P_T(X)$ (GeV/c)	$P_T(B)$ (GeV/c)	$c\tau$ (μm)	Signal Window (GeV/c^2)	Sideband Window (GeV/c^2)
			Selection Quantity		
$B^- \to J/\psi\ K^-$	2	8	100	5.22 − 5.32	5.4 − 5.8
$B^0 \to J/\psi\ K^*$	3	8	100	5.22 − 5.32	5.4 − 5.8
$B^0_s \to J/\psi\ \phi$	2	6	positive	5.32 − 5.42	5.5 − 5.9
K^* within $\pm$ 50 MeV/c^2 of 896.1 MeV/c^2					
ϕ within $\pm$ 10 MeV/c^2 of 1019.4 MeV/c^2					

Table 1: Final selection criteria used to reconstruct B mesons. Also shown are the mass windows used to define the B meson signal and sideband regions.

6 Mass Determination

Figure 6 show the reconstructed decays (a) $B^- \to J/\psi \ K^-$ and (b) $B^0 \to J/\psi \ K^*$ using the selection criteria of Tab. 1. Figure 7 similarly shows the reconstructed decay $B_s^0 \to J/\psi \ \phi$.

6.1 Mass Fits

The data in Figures 6 and 7 are fit (excluding the region one pion mass below the respective peaks) using an unbinned likelihood fit assuming a Gaussian signal on a linear background. In the fit, the calculated mass uncertainty of a given candidate, obtained by propagating the track parameter uncertainties (already multiplied by 1.8), is scaled by an additional factor of 1.3 to obtain agreement with the observed mass resolution. We find 147 ± 14 B^- candidates at a mass of 5279.1 ± 1.7 MeV/c^2, 51 ± 8 B^0 candidates at a mass of 5281.3 ± 2.2 MeV/c^2, and 32 ± 6 B_s^0 candidates at a mass of 5369.9 ± 2.3 MeV/c^2. Performing a binned likelihood fit to a linear background and Gaussian signal shape gives measured resolutions of 14.4 ± 1.6 MeV/c^2 for B^-, 11.5 ± 1.9 MeV/c^2 for B^0, and 10.4 ± 2.6 MeV/c^2 for B_s^0.

6.2 Systematic Uncertainties

Systematic uncertainties on the mass measurement arise from several sources. Each effect has been studied with signal and sideband events of all three reconstructed B mesons. To the precision that the systematic uncertainty is quoted, the effect is the same for all three states unless otherwise noted.

6.2.1 Measurement Uncertainties of the Track Parameters

The covariance matrix which describes uncertainties of the individual fitted track parameters is corrected by a multiplication factor of 1.8. This scale factor has been varied in magnitude and varied asymmetrically between the transverse and longitudinal track parameters. In these studies, no systematic shift in B meson masses are seen. Variations in the fitted mass were seen if the mass uncertainty scale factor, nominally 1.3, was varied between 1.0 and 1.5. The maximum effect over all three resonances was 0.3 MeV/c^2 which is taken as a common systematic due to our incomplete understanding of the uncertainties on measured track parameters.

6.2.2 Selection Criteria

Each of the selection criteria for each of the states is varied to study possible systematic effects. Over a large range of P_T cuts, $c\tau$ and CL(χ^2) requirements, and the mass window used to define the daughter meson, no statistically significant systematic is observed.

6.2.3 $\Delta \cot \theta$

The effect of the scaling $\cot \theta$ by 0.9985 ± 0.008 was studied by applying the extreme range of the $\cot \theta$ scale to tracks of B candidates and sideband events. The mean of the event-by-event mass differences for the B^-, B^0, and B_s^0 mesons allow the assignment of systematic uncertainties of $0.8 \ \text{MeV}/c^2$, $0.9 \ \text{MeV}/c^2$, and $0.6 \ \text{MeV}/c^2$ respectively.

6.2.4 Momentum Scale

The momentum of tracks are corrected for energy losses as the tracks propagate through material of the detector. Because this correction is highly correlated with an overall P_T scale correction, the uncertainty in the dE/dx correction is incorporated in the overall transverse momentum scale uncertainty of 0.02%. The momentum scale has been varied within the range of $\pm$ 0.02% and the corresponding event-by-event mass shift of B meson candidates has been studied. At the extreme ranges of the P_T scale, each of the B meson candidates shift $0.4 \ \text{MeV}/c^2$ which is taken as the systematic.

6.2.5 Checks at Low P_T

The P_T distribution of K candidates from ϕ decay for the B_s^0 candidates begins at $\sim 0.7 \ \text{GeV}/c$. At issue is whether there is a possible P_T dependent systematic at low P_T. Since muons in $J/\psi \to \mu^+ \ \mu^-$ decays have P_T above $1.4 \ \text{GeV}/c$ we make further checks to insure that there is no systematic present at lower transverse momentum. We check for this effect using two samples. The decay $\psi(2S) \to J/\psi \ \pi^+ \ \pi^-$ is reconstructed with $P_T(\pi)$ beginning at $0.4 \ \text{GeV}/c$ where our track reconstruction begins to become efficient. Fig. 8 shows the reconstruction of $\psi(2S)$ using a vertex constraint and dimuon mass constraint when requiring the di-pion mass to be between 0.45 and $0.58 \ \text{GeV}/c^2$ and $\text{CL}(\chi^2) > 1\%$. The fitted mass value of $3685.9 \pm 0.2 \ \text{MeV}/c^2$ agrees with the world average of $3686.00 \pm 0.09 \ \text{MeV}/c^2$ [17]. We also note that either the K or π in K^* decays for B^0 candidates have P_T below $2.0 \ \text{GeV}/c$ approximately 50% of the time. Since the reconstructed B^0 mass is also in agreement with its world average, we assign no additional systematic uncertainty on the momentum scale at low P_T.

6.2.6 Other Systematics Effects

Using the large statistics sample of $J/\psi \to \mu^+ \ \mu^-$ decays, systematic effects such as the precision to which the momentum scale is known on average can be quantified. In addition, residual systematic effects such as the dependence on $\Delta \cot \theta$ have been corrected. The resulting systematic effects on B_s^0 mass determination from these sources is small $(0.7 \ \text{MeV}/c^2)$. However, there are non-Gaussian tails in many of the tracking distributions. Further, we lack a full understanding of the covariance matrix. We can set a conservative estimate of remaining possible systematics from the fact that the mass difference between B^- and B^0 has been measured to be $0.34 \pm 0.29 \ \text{MeV}/c^2$ [16]). We measure a consistent mass difference of $2.2 \pm 2.8 \ \text{MeV}/c^2$. We can use the $2.8 \ \text{MeV}/c^2$ statistical uncertainty as a conservative estimate for other unaccounted systematic effects. To improve

the statistical power of our estimate, we consider B sideband track combinations which are kinematically consistent with coming from one of the three decays and which are consistent with coming from the primary vertex. By comparing the constrained fit and unconstrained fit masses for these events (*i.e.* how much the constrained fit moves the mass is a measure of how much a systematic could affect the mass), we find the statistical precision to which we see no systematic shift to be approximately 1 MeV/c^2. We assign this 1 MeV/c^2 systematic to account for possible mass shifts due to effects which are not yet understood.

7   Conclusion

The following decays have been fully reconstructed: $B^- \to J/\psi \ K^-$, $B^0 \to J/\psi \ K^*$, and $B_s^0 \to J/\psi \ \phi$. In each case, the $J/\psi \to \mu^+ \ \mu^-$ decay is used to allow the event to be recorded for analysis. The mass of each state is determined using an unbinned likelihood fit. Several sources of systematic uncertainty are summarized in Tab. 2.

Systematic Effect	B^-	B^0	B_s^0
Covariance Matrix	0.3	0.3	0.3
$\Delta\cot\theta$ Effect	0.8	0.9	0.6
Momentum Scale	0.4	0.4	0.4
dE/dx Material Composition	(included in above)		
Other Effects	1.0	1.0	1.0
Total MeV/c^2	1.4	1.4	1.3

Table 2: Summary of the contributions to the systematic uncertainties in the B meson measured masses.

The measured masses of the B^-, B^0, and B_s^0 mesons are shown in Tab. 3.

B Meson	Measured Mass (MeV/c^2)	Statistical Uncertainty	Systematic Uncertainty
B^-	5279.1	1.7	1.4
B^0	5281.3	2.2	1.4
B_s^0	5369.9	2.3	1.3

Table 3: Summary of the measured B meson masses.

The difference between this result and our previous published value [4] of the B_s^0 mass has been studied in detail and results primarily from statistical fluctuations.

Taking the systematic uncertainties associated with the momentum scale and $\Delta\cot\theta$ as common systematics, we calculate the mass difference between the B_s^0 meson and B_L which is defined as the average of the measured B^- and B^0 states. We derive a mass difference of $89.7 \pm 2.7 \pm 1.2$ MeV/c^2.

8   Acknowledgements

References

[1] References to a specific charge state should be implied to pertain also to the charge conjugate state.

[2] M. Mangano and P. Nason. Nucl. Phys. B373, 295 (1992)

[3] CDF Collaboration, F. Abe *et al.*, Proceedings of the 27th International Conference on High Energy Physics, University of Glasgow, Glasgow, Scotland, FERMILAB-CONF-94/141-E, 1994.

[4] CDF Collaboration, F. Abe *et al.*, Phys. Rev. Lett. 71, 1685 (1993).

[5] Particle Data Group, Phys. Rev. D **50**, 1639 (1994).

[6] DELPHI Collaboration, P. Abreau *et al.*, Phys. Lett. **B324**, 500 (1994); ALEPH Collaboration, D. Buskulic *et al.*, Phys. Lett. **B316**, 631 (1993) and Phys. Lett. **B311**, 425 (1993); OPAL Collaboration, P. T. Acton *et al.*, Phys. Lett **B295**, 357 (1992).

[7] CDF Collaboration, F. Abe *et al.*, Nucl. Instrum. Methods Phys. Res., Sect. A **271**, 387 (1988); F. Bedeschi *et al.*, Nucl. Instrum. Methods Phys. Res., Sect. A **268**, 50 (1988); G. Ascoli *et al.*, Nucl. Instrum. Methods Phys. Res., Sect. A **268**, 33 (1988).

[8] CDF Collaboration, F. Abe *et al.*, Phys. Rev. **D50**, 2966 (1994).

[9] D. Amidei *et al.*, Nucl. Instrum. Methods Phys. Res. , Sect. A **350**, 73 (1994)

[10] In CDF, ϕ is the azimuthal angle, θ is the polar angle and r is the radius from the proton beam axis (z axis).

[11] Particle Data Group, Phys. Rev. D **50**, 1644 (1994).

[12] C. Newman-Holmes, E. E. Schmidt, and R. Yamada, Nucl. Instrum. Methods Phys. Res. , Sect. A **274**, 443 (1989).

[13] F. Abe *et al.*, FERMILAB-PUB-95/003-E, submitted to Phys. Rev. **D**, (1995).

[14] Particle Data Group, Phys. Rev. D **50**, 1662 (1994).

[15] F. Abe *et al.*, FERMILAB-PUB-94/420-E. submitted to Phys. Rev. Lett., (1994); F. Abe *et al.*, Phys. Rev. Lett. **72**, 3456 (1994)

[16] Particle Data Group, Phys. Rev. D **50**, 1622 (1994).

[17] Particle Data Group, Phys. Rev. D **50**, 1656 (1994).

CDF

y

θ φ

z
(EAST)

x

CMX

CMP

SOLENOID RETURN YOKE

CMU

FMU

1 METER

WHA

CHA

CEM   SOLENOID

FHA

PHA

CDT

FEM

CTC

BBC
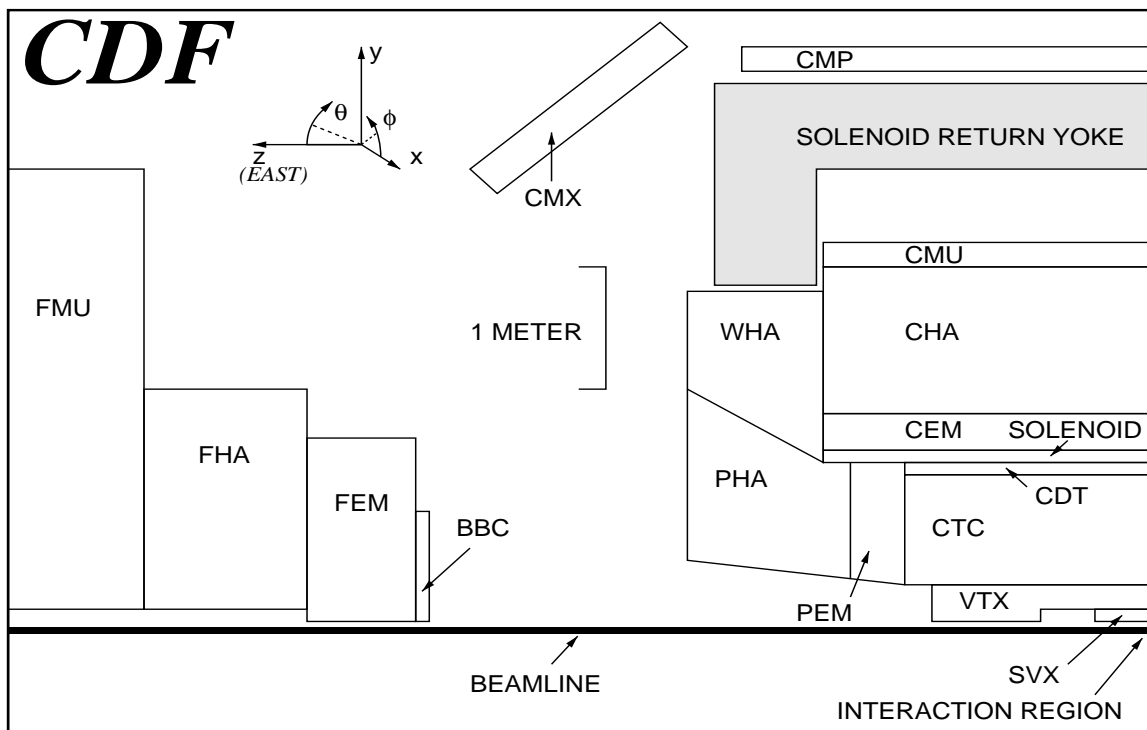
VTX

PEM

SVX

BEAMLINE

INTERACTION REGION

Figure 1: Side view representation of the CDF detector used in the 1992–1993 run.
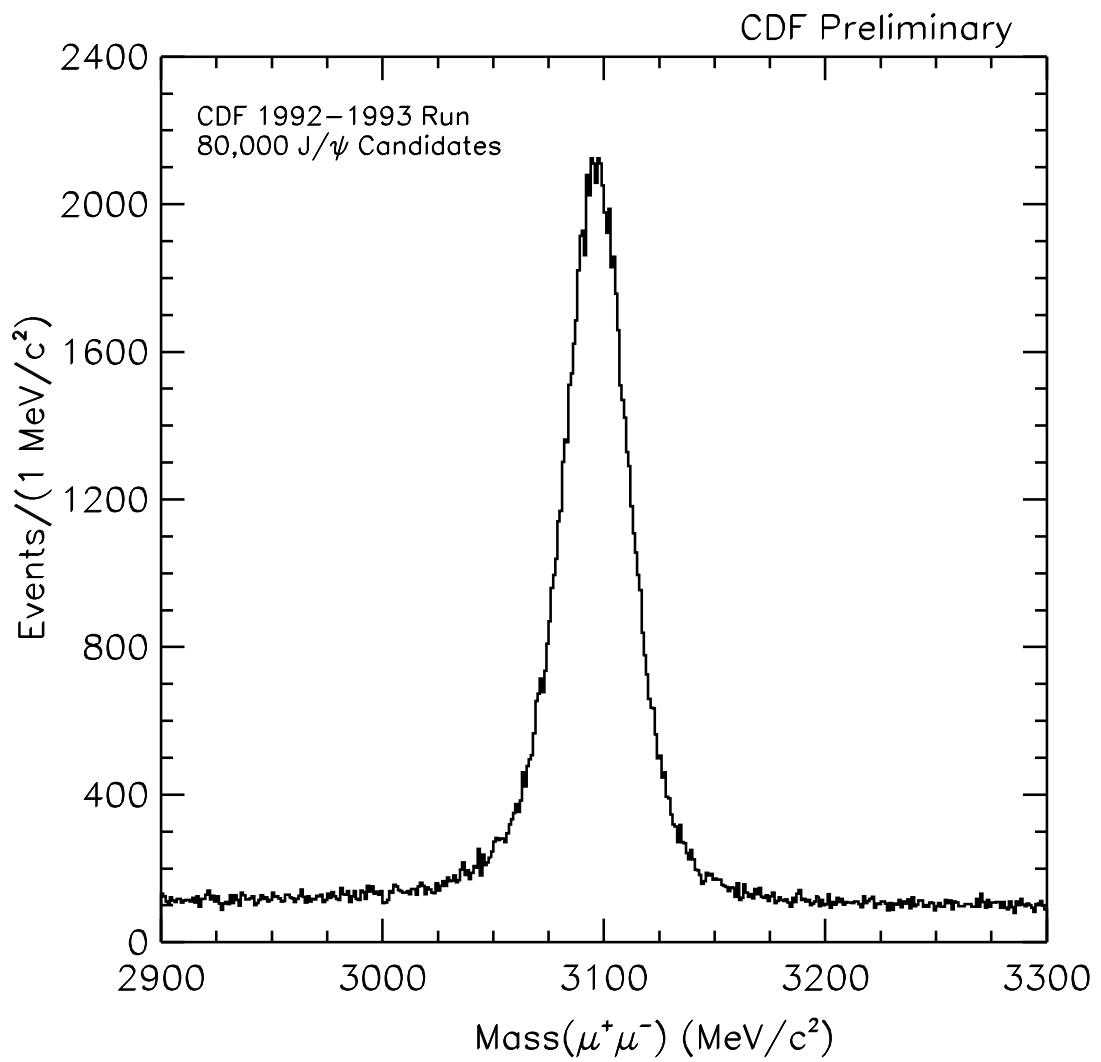
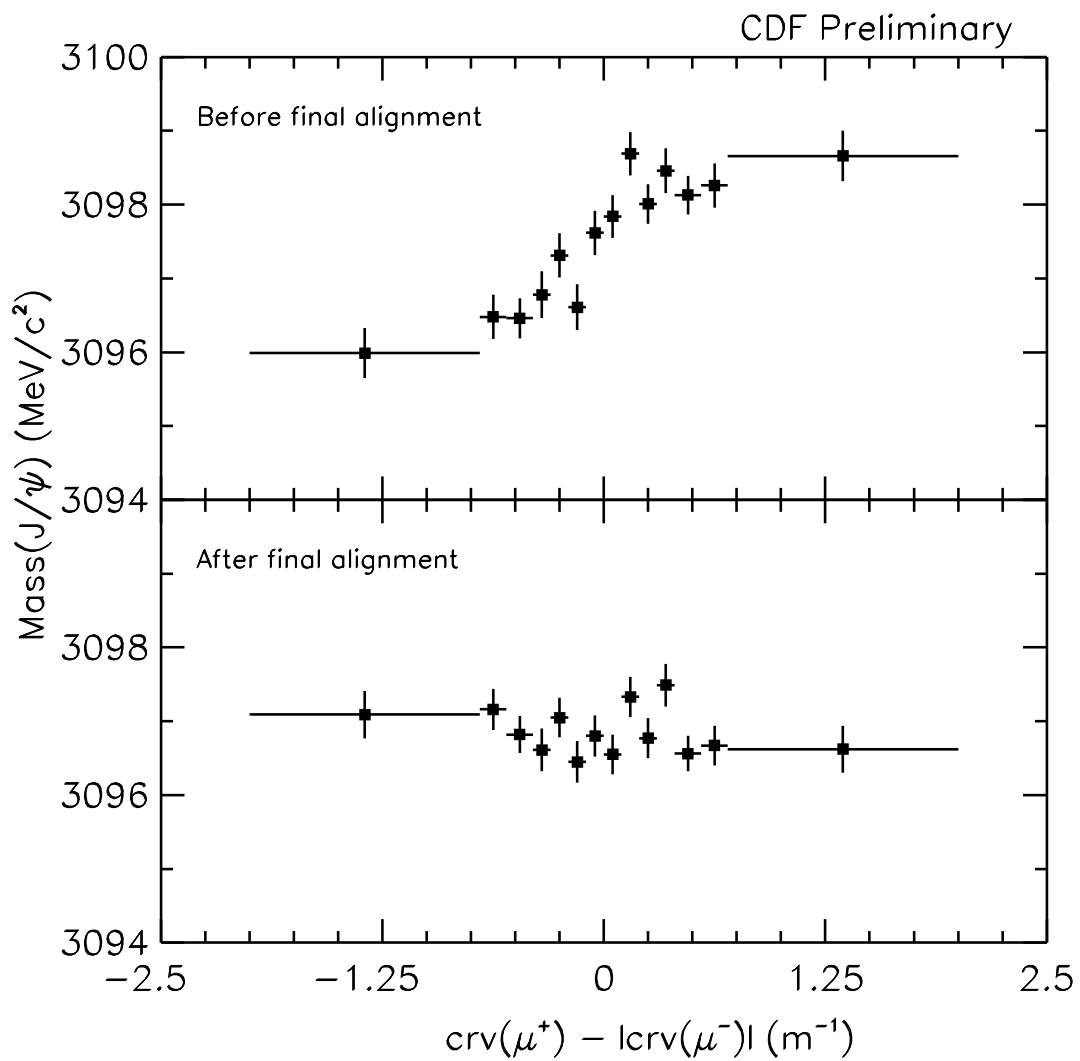Figure 2: Dimuon mass distribution from the CDF 1992–1993 run.

Figure 3: False curvature tracking systematic effect observed when the J/ψ mass is plotted versus the difference in absolute curvature for the positive and negative muons. The effect is removed upon applying alignment corrections as used for the tracks in this analysis.
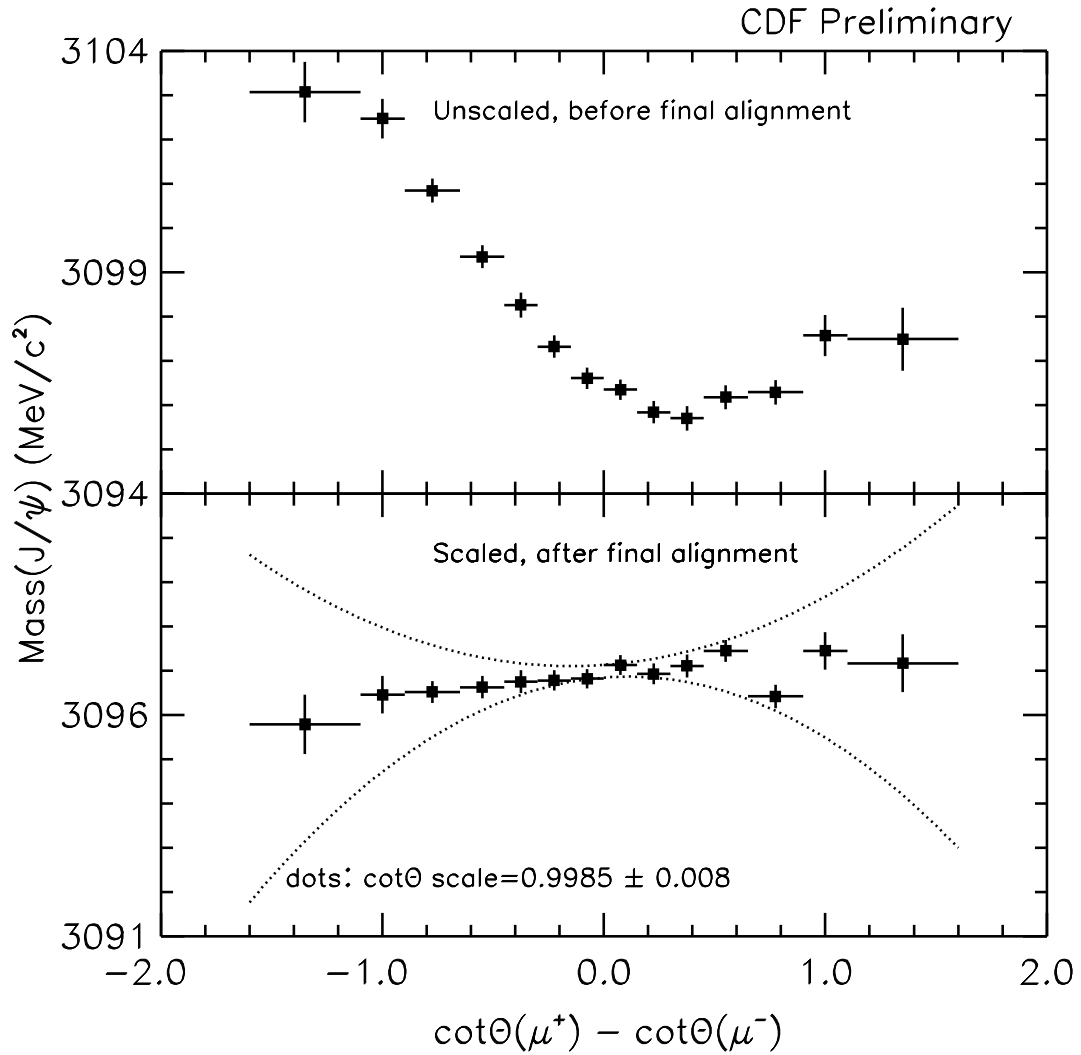
Figure 4: A systematic effect observed when the J/ψ mass is plotted versus the difference in the $\cot\theta$ between the two muons. The effect is mitigated after final CTC alignment and after scaling $\cot\theta$ by 0.9985 $\pm$ 0.008. The dotted lines show the effect at the extreme bounds of the scale factor used for determining systematic uncertainties.
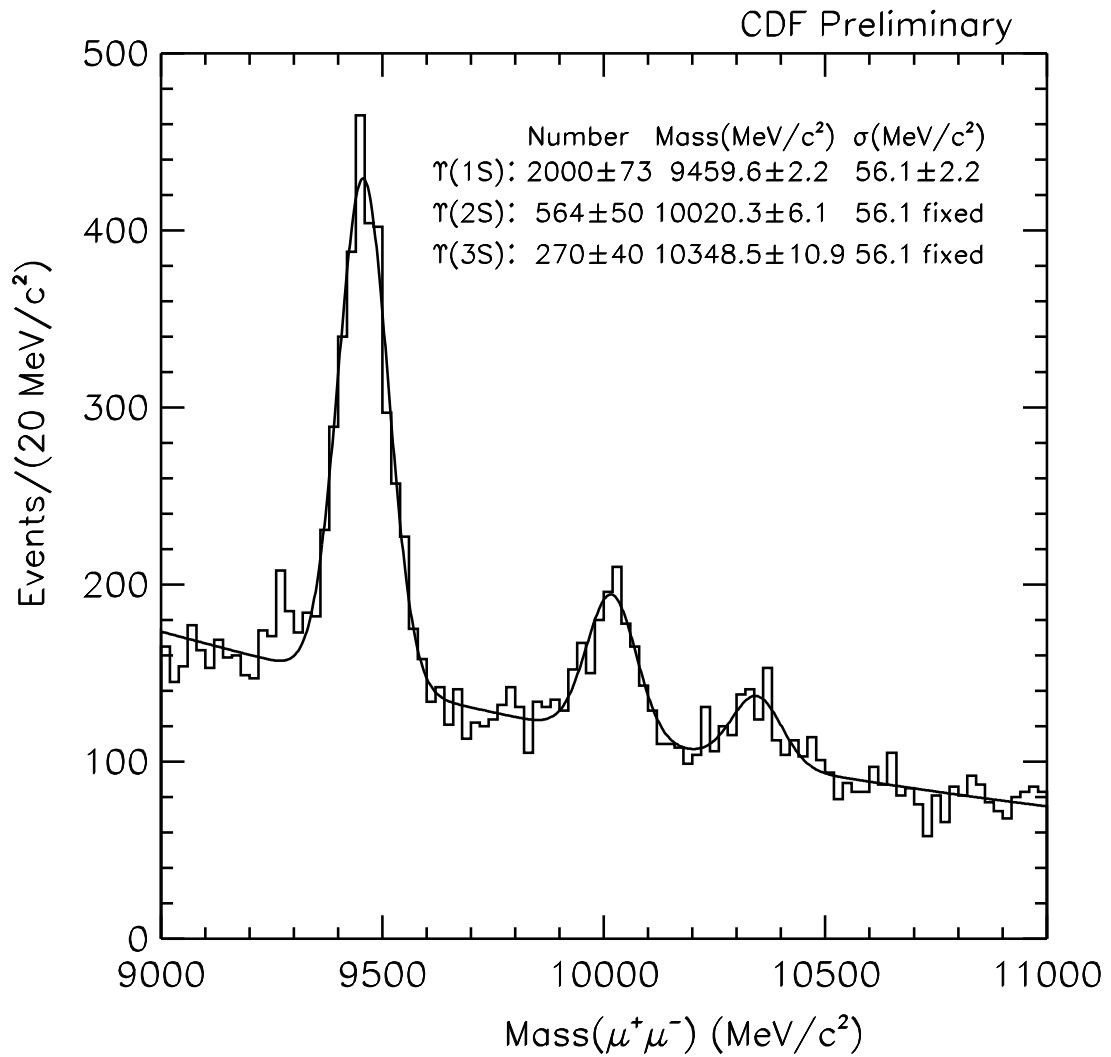
Figure 5: Reconstruction of $\Upsilon \rightarrow \mu^+ \mu^-$ after applying all corrections and scale factors used to set the $J/\psi \rightarrow \mu^+ \mu^-$ peak at the J/ψ mass. All Υ states agree within the statistical uncertainty to the world average masses.
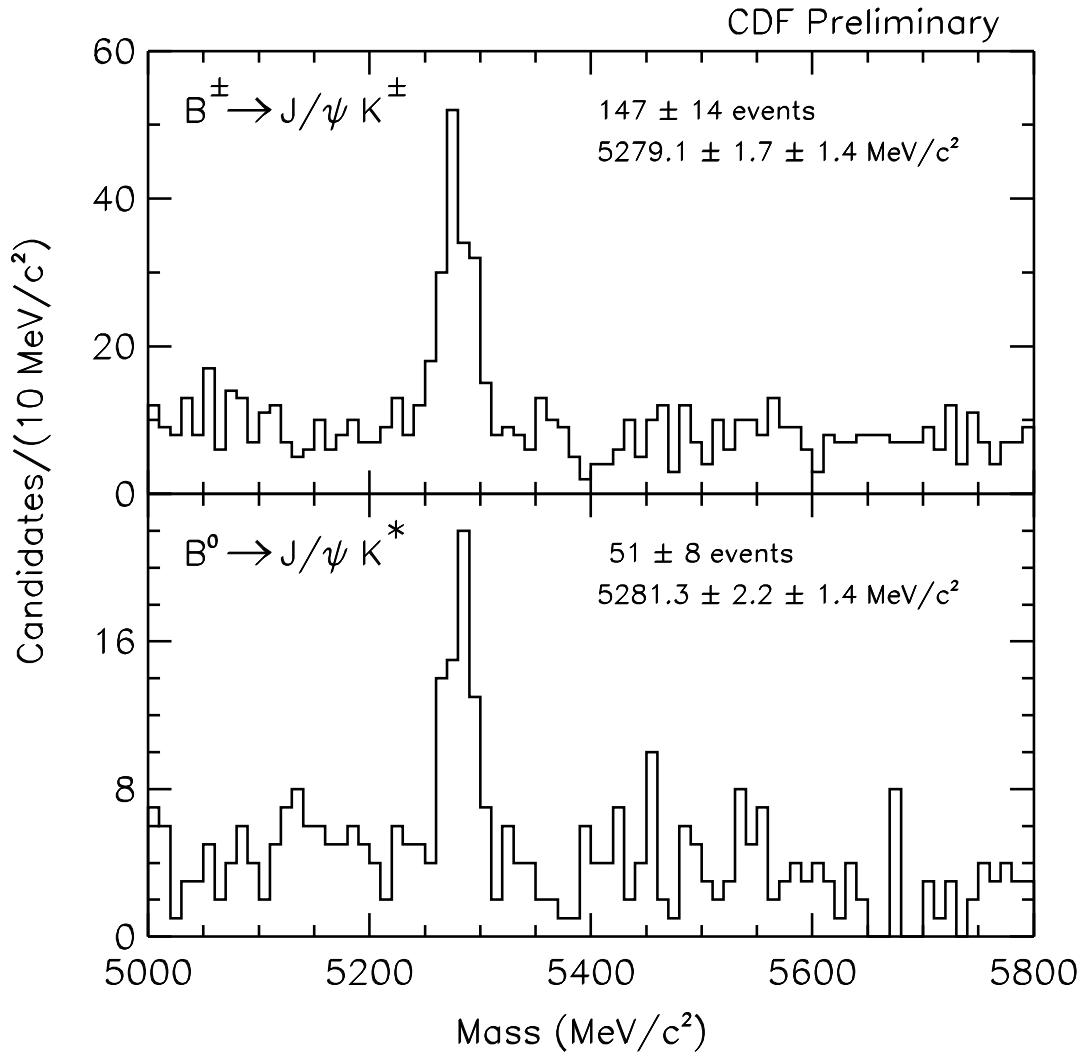
Figure 6: (a) $J/\psi\ K^-$ mass distribution and (b) $J/\psi\ K^*$ mass distributions for the events passing the B^- and B^0 selection criteria. The mass is determined by an unbinned likelihood fit of a Gaussian signal and a linear background. The quoted systematic uncertainty is evaluated within the text.
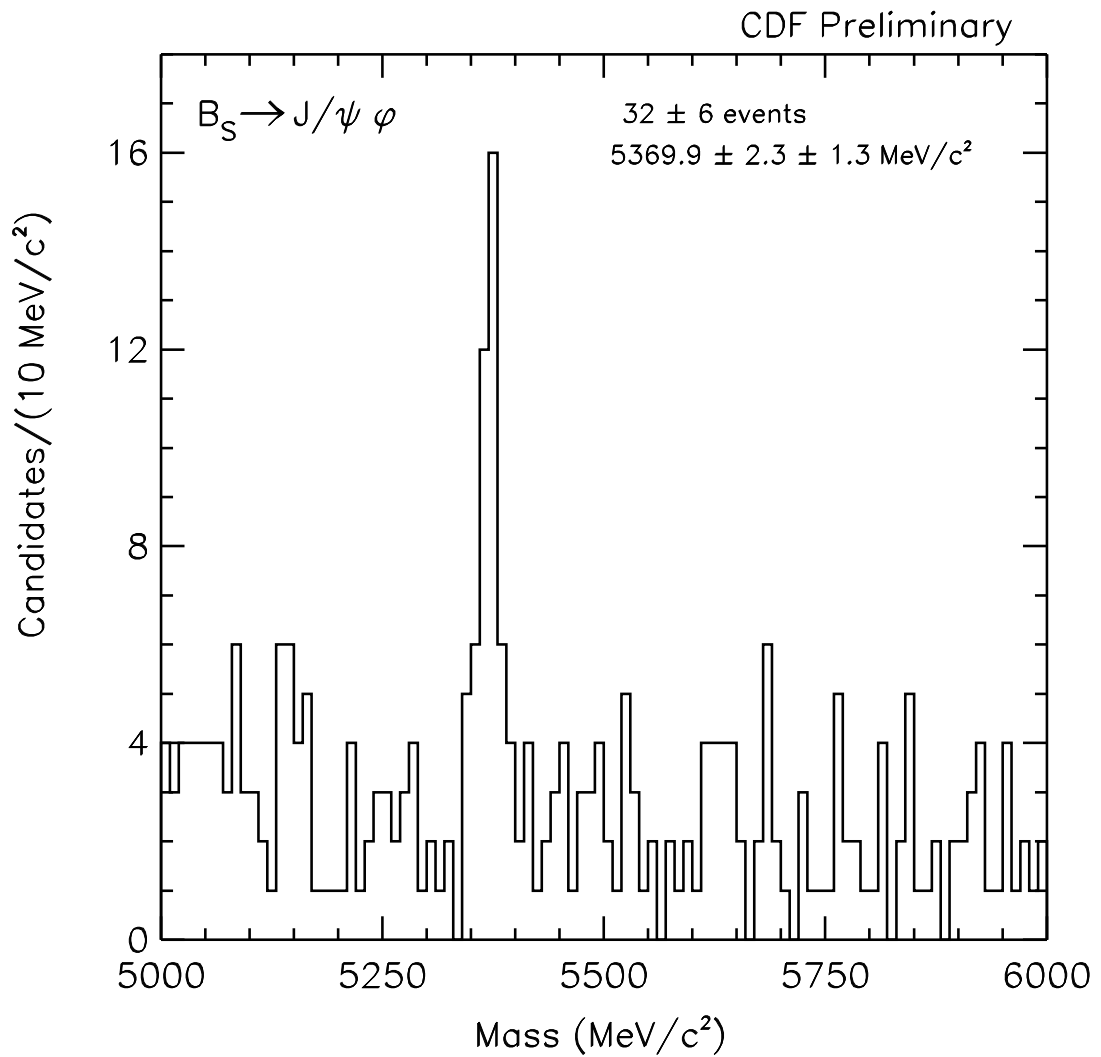
Figure 7: $J/\psi\ K^+K^-$ mass distribution for the events passing the B_s^0 selection criteria. The mass is determined by an unbinned likelihood fit of a Gaussian signal and a linear background. The quoted systematic uncertainty is evaluated within the text.
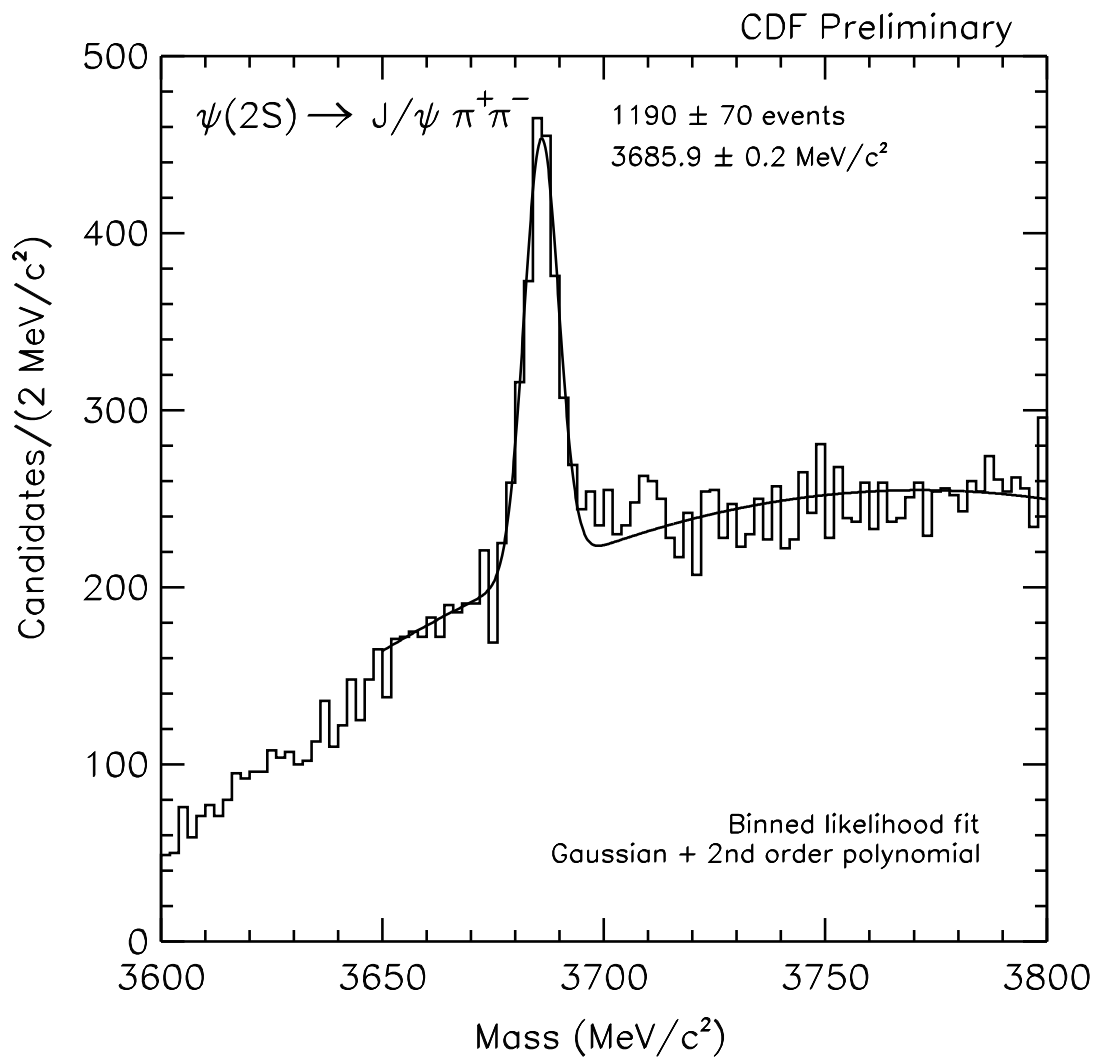
Figure 8: Mass distribution for the reconstruction of $\psi(2S) \to J/\psi \ \pi^+ \ \pi^-$.